European Journal of Pharmaceutics and Biopharmaceutics 78 (2011) 385–393

Contents lists available at ScienceDirect

European Journal of Pharmaceutics and Biopharmaceutics

journal homepage: www.elsevier.com/locate/ejpb

Research paper

Improvement of oxaprozin solubility and permeability by the combined use of cyclodextrin, chitosan, and bile components

F. Maestrelli [a], M. Cirri [a], N. Mennini [a], N. Zerrouk [b], P. Mura [a,*]

[a] Department of Pharmaceutical Sciences, University of Florence, Sesto Fiorentino, Italy
[b] Lab. de Pharmacotechnie et Biopharmacie, Faculté de Sciences Pharmaceutiques et Biologiques, Université René Descartes, Paris, France

ARTICLE INFO

Article history:
Received 14 January 2011
Accepted in revised form 14 March 2011
Available online 23 March 2011

Keywords:
Oxaprozin
Solubility
Permeability through Caco-2 cells
Bile components
Cyclodextrin
Chitosan

ABSTRACT

The effect of the combined use of randomly methylated β-cyclodextrin (RAMEB), chitosan (CS), and bile components (dehydrocholic (DHCA) or ursodeoxycholic (UDCA) acids and their sodium salts) on solubility and permeability through Caco-2 cells of oxaprozin (a very poorly water-soluble non-steroidal anti-inflammatory drug) has been investigated. Addition of CS, bile acids, and their sodium salts increased the RAMEB solubilizing power of 4, 2, and 5 times, respectively. Drug–RAMEB–CS co-ground systems showed very higher dissolution rate than corresponding drug–RAMEB systems. Addition of bile components further improved drug dissolution rate. The CS presence enabled a significant increase in drug permeability through Caco-2 cells with respect to drug–RAMEB systems. Moreover, CS and NaDHC showed a synergistic enhancer effect, enabling a 1.4-fold permeability increase in comparison with systems without bile salt. However, unexpectedly, no significant differences were found between physical mixtures and co-ground products, indicating that drug permeation improvement was due to the intrinsic enhancer effect of the carriers and not to drug-carrier interactions brought about by co-grinding, as instead found in dissolution rate studies. The combined use of RAMEB, CS, and NaDHC could be exploited to develop effective oral dosage forms of oxaprozin, with increased drug solubility and permeability, and then improved bioavailability.

1. Introduction

Dissolution rate in gastrointestinal fluids and permeability through biological membranes are considered as the most important factors in determining the bioavailability of orally administered drugs [1–3]. In spite of their potentially good therapeutic efficacy and low toxicity, a high percentage of drug candidates are destined to fail in preclinical and clinical phase due to inadequate absorption properties [4,5]. In particular, it is estimated that the percentage of poorly soluble substances coming from combinatorial chemistry research and/or from biologically based high-throughput screening is up to 60% of the total, and it is progressively increasing [6]. The development of effective carrier systems capable of overcoming such problems, and thus increasing bioavailability of these drugs, is gaining increasing attention and is a crucial challenge for industry and academia institutions, especially due to the difficulties encountered over the last years in the area of drug discovery. Moreover, also already well-known active pharmaceutical ingredients could exploit the beneficial effect of these carriers, obtaining an improvement of their biopharmaceutical properties and thus of their therapeutic effectiveness.

Oxaprozin [3-(4,5-diphenyl-1,3-oxazol-2-xyl) propionic acid] is a non-steroidal anti-inflammatory drug, mainly used for the treatment of inflammatory disorders such as, in particular, osteoarthritis and rheumatoid arthritis. Oxaprozin belongs to the Class II of the Biopharmaceutics Classification System (BCS), since it is a highly permeable but very low soluble drug [7]. Moreover, in spite of its acidic nature and differently from most of the other acidic NSAIDs, it complies with the BCS low solubility criteria over the entire pH range from 1.2 to 7.4 [7]. Therefore, a proper improvement of oxaprozin solubility, possibly succeeding in obtaining its promotion to Class I drugs, is particularly advisable. In fact, the enhancement of drug dissolution rate would enable to increase its absorption rate and bioavailability, and reduce its dosage, thus reducing the risk of adverse cardiovascular and/or gastrointestinal events [8].

With this aim, in a previous work, we studied and compared the effectiveness of several cyclodextrins in improving oxaprozin dissolution properties, and the randomly methylated β-cyclodextrin (RAMEB) was selected as the best one [9]. However, it is known that the pharmaceutical use of cyclodextrins, and particularly of the methylated ones, is limited, mainly by problems of potential toxicity [10]. Therefore, it should be useful to increase their

* Corresponding author. Department of Pharmaceutical Sciences, University of Florence, Via Schiff 6, Sesto Fiorentino, 50019 Florence, Italy. Tel.: +39 055 4573672; fax: +39 055 4573673.
E-mail address: paola.mura@unifi.it (P. Mura).

0939-6411/$ - see front matter © 2011 Elsevier B.V. All rights reserved.
doi:10.1016/j.ejpb.2011.03.012

solubilizing effect by the addition of suitable auxiliary substances, in order to reduce the amount of cyclodextrin to use [11–14].

Chitosan [(1 → 4)-2-amino-2-deoxy-β-d-glucan] is a cationic polysaccharide of natural origin obtained by *N*-deacetylation of chitin, resulting in a copolymer of *N*-acetyl-d-glucosamine and d-glucosamine [15]. It is presently in development as a safe excipient in drug formulations in virtue of its high biocompatibility, biodegradability, and lack of toxicity associated with bioadhesiveness, dissolution, and permeation enhancer properties [15–17]. Furthermore, its antiacid and antiulcer activities can be exploited to reduce gastric irritation caused by active compounds, such as anti-inflammatory drugs [18]. Finally, a synergistic effect of cyclodextrin and chitosan in improving solubility and/or permeation properties of some drugs has been recently shown [19–21], indicating such a polymer as a good potential partner of cyclodextrins.

Bile acids and their salts are biocompatible biosurfactants, widely used as carriers for hydrophobic drugs in virtue of their dissolution and permeation enhancer properties [22–24]. However, it should be also noticed that, above their critical micellar concentration (CMC), bile acids can associate with phospholipids of cell membranes, causing a membranolytic effect which is directly related to the intensity of their enhancer effect [25,26]. Otherwise, their combined use with other suitable components, such as, for example, fatty acids, phospholipids, or polyamines, improved their effectiveness and allowed a reduction in their concentration, thus lowering risks of toxicity toward the intestinal mucosa [27–29].

On the basis of all these considerations, the purpose of the present study was to investigate the potential advantages of the combined use of cyclodextrin, chitosan, and bile components (dehydrocholic and ursodeoxycholic acids and their sodium salts), with the aim of better exploiting their favorable carrier properties and evaluating their possible synergistic effects on dissolution and absorption behavior of oxaprozin.

2. Materials and methods

2.1. Materials

Oxaprozin (OXA) (Mw 293.3, p*K*a 4.3, melting point 162–163 °C, log *P* 4.8 at pH 7.4 [30]) (Fig. 1) was kindly donated by S.I.M.S. (Incisa Valdarno, Florence, Italy) and used as received. Amorphous randomly substituted methyl-β-cyclodextrin (RAMEB), with an average molar substitution degree per anhydroglucose unit of 1.8, was a gift from Wacker-Chemie GmbH (München, Germany). Chitosan (CS) (molecular weight 150,000, deacetylation degree 75–85%) was from Sigma Aldrich (St. Louis, USA). Dehydrocholic acid (DHCA), ursodeoxycholic acid (UDCA), and sodium dehydrocholate (NaDHC) were from Polichimica (Bologna, Italy), and sodium ursodeoxycholate (NaUDC) from Prod. Chimici e Alimentari (Alessandria, Italy). Solvents used in the HPLC procedure were of HPLC grade. All other reagents were of analytical grade.

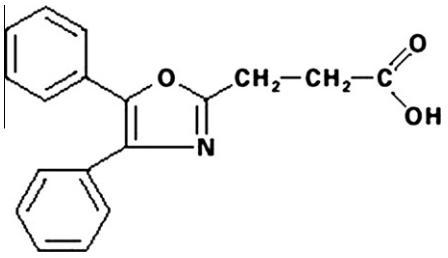

Fig. 1. Chemical structure of oxaprozin (4,5-diphenyl-2-oxazole-propionic acid).

2.2. Phase solubility studies

Phase solubility studies were performed by adding an excess of drug (60 mg) to 10 mL of pH 5.5 phosphate buffer solutions containing increasing concentrations (0–5–10–15–20–25 mM) of RAMEB, alone or in the presence of a fixed amount of CS (0.0625% w/v) and/or each of the selected bile components (2.5 mM). The CS amount was selected according to previous studies that showed no cellular toxicity until this concentration [21]. The bile components concentration was maintained under their CMC, to avoid risks of toxicity [28]; the CMC values for NaDHC and NaUDC are 10 and 20 mM, respectively [31] and for DHCA and UDCA 6 and 7 mM, respectively [32]. Glass containers were sealed preserved from the light and electromagnetically stirred (500 rpm) at constant temperature (25 °C). Aliquots were withdrawn every 24 h until equilibrium (72 h), filtered (0.45-μm pore size), and assayed for drug content by HPLC as described below. No detectable pH variations of the solutions were observed after the 72 h. Each test was performed in triplicate (coefficient of variation (CV) < 3%). The apparent binding constants of OXA–RAMEB complexes were calculated from the slope of the straight lines of the phase solubility diagrams [33].

2.3. Preparation of solid systems

Equimolar binary (OXA–RAMEB) or ternary (OXA–RAMEB–bile component) solid systems, added with a fixed amount of CS (0.0625% w/w), were prepared by different methods. Physical mixtures (PM): obtained by 15 min tumble mixing weighed amounts of simple components (75–150 μm sieve fraction). Co-ground products (GR): by ball-milling PM 30 min at 24 Hz (high energy vibrational micro mill Mixer Mill MM 200, Retsch GmbH, Düsseldolf, Germany). Coevaporated products (COE): by coevaporation in a rotary evaporator (Laborota 4000, Heidolph Milano, Italy) of a 1:1 v/v EtOH–water solution (added of 5% v/v acetic acid) of PM. Kneaded products (KN): by adding a small volume of EtOH to the PM, kneading thoroughly with a pestle to obtain homogeneous slurry and continuing until all the solvent was removed. Sealed-heated products (SH): by heating PM in sealed glass containers at 90 °C for 2 h, added of 10 μL of bidistilled water.

2.4. Characterization of solid systems

The physicochemical and morphological properties of pure components and of their different examined combinations were investigated by differential scanning calorimetry (DSC) and scanning electron microscopy (SEM) studies.

DSC analyses were performed with a Mettler TA4000 Star^e system (Mettler Toledo, Milano, Italy) apparatus equipped with a DSC 25 cell on 5–10 mg samples (Mettler M3 Microbalance) scanned in pierced aluminum pans at 10 °C/min between 30 and 200 °C under static air. The instrument was calibrated using Indium as a standard (99.98% purity; melting point 156.61 °C; fusion enthalpy 28.71 J g^{-1}).

SEM photographs were recorded on a S-250 Hitachi (Paris, France) scanning electron microscope. Prior to examination, samples were gold sputter-coated to render them electrically conductive using a fine coat ion sputter JFC-1100 JEOL.

2.5. Dissolution rate studies

Dissolution rate studies of OXA, alone and from the different systems, were performed at 37 °C in pH 5.5 phosphate buffer solution according to the dispersed amount method [9]. Briefly, 50 mg of drug or drug equivalent was added to 75 mL of solvent in a 150-mL beaker preserved from the light and stirred

(100 rpm) with a glass three-blade propeller. At time intervals (2, 5, 10, 20, 30, 40, 50, 60 min), aliquots were withdrawn, filtered (0.45-μm pore size), and assayed for drug content by HPLC as described below. It was verified that OXA did not absorb to the filter used for the separation of solid. A correction was calculated for the cumulative dilution caused by sample replacement with an equal volume of fresh medium. Each test was repeated four times (CV < 2.5%). Dissolution was characterized through the percent of drug dissolved after 10 min ($DP_{10\%}$), as an index of the rate of dissolution, and the dissolution efficiency at 60 min (DE_{60}), as an index of the totality of the process. DE_{60} was calculated according to the following equation [34]:

$$DE = \frac{\int_{t_2}^{t_1} y \cdot dt}{y_{100} \cdot (t_2 - t_2)} \cdot 100 \quad (1)$$

where y is the percentage of dissolved product. DE is then the area under the dissolution curve between time points t_1 (0 min) and t_2 (60 min) (measured using the trapezoidal rule), expressed as a percentage of the area of the rectangle described by 100% dissolution in the same interval time ($y_{100} \cdot (t_1 - t_2)$).

The dissolution profile of the plain drug was compared with those from its different combinations with the examined carriers by using the following ratio test procedures [35]: ratio of $DP_{10\%}$ and ratio of $DE_{60\%}$ (each value was calculated by the ratios of the respective $DP_{10\%}$ and $DE_{60\%}$values obtained for plain OXA and the other tested products).

2.6. Storage stability studies

Samples of selected drug–RAMEB–CS systems, in the presence or not of bile salts, were stored for one year in closed glass vials, preserved from the light, in an air-conditioned room controlled for temperature (25 ± 1 °C) and relative humidity (RH 50%). Every 30 days aliquots were withdrawn and subjected to DSC analysis and dissolution studies.

2.7. Cell cultures

The Caco-2 cell line was generously given by Dr. A. Zweibaum and Dr. M. Rousset (INSERM U170,Villejuif, France). Cells were grown routinely in T-flasks at 37 °C in a 10% CO_2/90% air atmosphere. The culture medium was a Dulbecco's modified Eagle's medium (DMEM, pH 7.4) containing 10% fetal bovine serum (FBS) and 1% non-essential amino acids (Vitrogen/Gibco TM Life Technologies, Cercy Pontoise, France). All cells were obtained at passage 8 and used at passages 80–85, according to previously published procedures [36,37]. The cells were seeded at a density of 0.9×10^6 cells/cm^2 on tissue culture-treated polycarbonate filters (area 4.71 cm^2) in Costar Transwell six-well plates (Costar Europe Ltd., Badhoevedorp, Netherlands). The culture medium, added with 110 IU/mL penicillin G, 10 μg/mL streptomycin sulfate, and 25 μg/mL Fungizone (Vitrogen/Gibco TM Life Technologies, Cercy Pontoise, France), was changed every second day, and cell cultures were kept at 37 °C in 10% CO_2/90% air atmosphere and 95% relative humidity. Filters were used for transport studies 21–28 days after seeding [38].

2.8. Transport studies

Test solutions consisted of 1×10^{-4} M OXA samples (alone or as physical mixture or co-ground system with RAMEB, CS, and NaDHC, prepared as described in Section 2.3) in Hanks' balanced salt solution (HBSS) added with 1% 4-morpholine-ethanesulfonic acid, adjusted at pH 5.5 with HCl 1 N, thermostated at 37 °C, and maintained under magnetic stirring until to complete dissolution. Yellow Lucifer (St. Quentin Fallavier, France), a hydrophilic fluorescent dye, was used to check the junction integrity of Caco-2 cell monolayer during the experiments. After filters preincubation at 37 °C in a 90% air–10% CO_2 atmosphere, 1.5 mL of test solution and 300 μL of the marker HBSS solution (3 mg/100 mL) were added to the apical (AP) side of cells (donor compartment) and 2.5 mL of HBSS solution to the basolateral (BL) one (acceptor compartment). At given intervals (30, 60, 90, 120, and 150 min), samples withdrawn from the basolateral side, replaced with an equal volume of fresh HBSS solution, were assayed for drug and marker content by HPLC, as described below. Results were corrected for dilution and given as cumulative transport as a function of time. Each experiment was performed in sextuple. The apparent permeability coefficient (Papp) was calculated using the following equation:

$$Papp = \frac{dQ}{dt} \cdot \frac{1}{A} \cdot \frac{1}{C_0} \quad (2)$$

where dQ/dt (μg/s) is the rate of drug appearance on the basolateral side, A the monolayer surface area and C_0 (μg/mL) the initial drug concentration in the donor compartment.

A mass balance calculation was carried out to determine whether accumulation or metabolism of the solute or adsorption to the apparatus occurred [39].

2.9. Measurement of the trans-epithelial electrical resistance (TEER)

TEER measurements were performed to evaluate possible cellular damage during experiments. TEER values were obtained by measuring the potential difference between the two sides of the cell monolayer with a Millicell® ERS meter (Millipore, Bedford, MA, USA) connected to a pair of chopstick electrodes [40]. Measurements started 10 min prior to incubation on the cells apical side with the test and blank solutions. All experiments were performed in sextuple in 90% air–10% CO_2 atmosphere at 37 °C. Mean TEER values for untreated monolayers were around 250 Ω cm^2.

2.10. Lactate dehydrogenase (LDH) cytotoxicity text

LDH test was used to assess the cytotoxicity of the tested carriers [41]. LDH leakage from Caco-2 cells was determined by the assay-kit of Roche diagnostics (Meylan, France). Briefly, the cells, after incubation in the wells, were washed with the Hanks' balanced salt solution and then added of 200 μL of medium containing the sample to be tested. The spontaneously released LDH from intact cells was considered as the low control (LC), while the high control (HC) was the enzyme released after cell lysis by addition of Triton®X-100 (1% v/v) solution. After incubation (120 min at 37 °C), 100 μL of supernatant was transferred from each well to a new plate and added of 100 μL of reconstituted reaction medium. After 30 min incubation at 37 °C, the enzymatic reaction was stopped by adding 50 μL/well of 1 N HCl solution. Absorbance at 490 nm was measured within 1 h with the ELISA reader. Cytotoxicity of the samples was calculated by the following equation:

$$\%\text{cytotoxicity} = \frac{A_s - A_{LC}}{A_{HC} - A_{LC}} \cdot 100 \quad (3)$$

where A_s is the absorbance for cells treated with the sample; A_{LC} and A_{HC} are the absorbance values of low control and high control, respectively.

2.11. High performance liquid chromatography (HPLC) assay

HPLC analyses were carried out with an Elite Lachrom Merck-Hitachi (Milano, Italy) apparatus equipped with an injector

valve with a 20-μL sample loop (Mod. Rheodyne) using a C_{18} Purosphere (5 μm 150 mm × 4.6 mm i.d.) column. The mobile phase was a mixture of pH 4 phosphate buffer: acetonitrile (60:40 v/v) [42]. The flow rate was 1.0 mL/min, and OXA was detected spectrometrically at 285 nm (retention time 3.8 min). The marker Lucifer Yellow was detected simultaneously, under the same experimental conditions (retention time 1.2 min).

2.12. Statistical analysis

Results of dissolution and permeation experiments were statistically analyzed by ANOVA (one-way analysis of variance) followed by the Student-Neuwman Keuls multiple comparison post-test (GraphPad Prism, version 4). The differences were considered statistically significant when $P < 0.05$.

3. Results and discussion

3.1. Phase solubility studies

As a preliminary step, solubility studies were carried out to evaluate the solubilizing power toward the drug of the different examined carriers, both alone and in combination, in the absence of RAMEB.

Bile acids and their salts were tested at 2.5 mM concentration. Such a concentration, lower than their CMC, was selected to avoid risks of toxicity, considering that the average concentration of bile components in human intestinal tract was reported to be 5–15 mM [43]. Moreover, their jointed use with other carriers should allow for reducing the dose necessary to manifest their enhancer effect [27–29]. As for the CS concentration, it was set at 0.0625% w/v according to previous studies that indicated absence of cellular toxicity until this polymer concentration [21].

Results of solubility studies indicated that all the considered carriers improved drug solubility, but only in a limited way, ranging from an about five times increase observed in the presence of bile acids drug to an about 11–12 times increase observed in the presence of CS or bile salts (Fig. 2). Moreover, combinations of CS with bile salts did not show any improvement in drug solubility with respect to their separated use, indicating the absence of any synergistic effect.

Phase solubility studies of RAMEB alone and in the presence of the different examined auxiliary substances, separately and/or in combination (all at the same concentrations as in the previous solubility studies), were then performed to investigate their influence on the cyclodextrin complexing and solubilizing properties. The obtained phase solubility diagrams showed in all cases linear curves classified as A_L-type according to Higuchi and Connors [33] (Fig. 3), which are considered indicative of the formation of soluble complexes of probable 1:1 mol:mol stoichiometry between drug and RAMEB, irrespective of the presence and type of added components.

The combined use of RAMEB with the other carriers showed in all case a synergistic effect on drug solubility improvement, which was clearly higher than the corresponding theoretical values given by the sum of the data obtained with the separated carriers. In fact, the OXA solubility increase ranged from a minimum of about 170 times (RAMEB–UDCA) up to more than 360 times (RAMEB–NaDHC–CS), with respect to the only about 60 times increase obtained with RAMEB alone. In particular, the presence of bile acids and even more of their sodium salts increased the RAMEB solubilizing efficiency toward the drug from a minimum of 2.2 times (for UDCA) up to about five times (for NaDHC), as appears from data in Table 1. This result, mainly imputable to the surfactant and solubilizing properties of bile components [23], reflected the different solubilizing power toward OXA of the examined bile components, previously observed in the absence of RAMEB (see Fig. 2). The better performance of sodium salts than the corresponding acids is attributable in both cases to their higher hydrophilicity and hydrosolubility. On the other hand, the better results obtained with NaDHC than with NaUDC could be related to their different affinities for interacting with OXA. However, the actual mechanism responsible for the observed findings remains to be elucidated, and it will be object of further studies. Moreover, the possible interaction between bile components and cyclodextrins should be also taken into account [44,45]. This could explain the observed reduction in the stability constant values of OXA–RAMEB complex (Table 1), as a consequence of a probable competition effect between drug and bile component for complexation with cyclodextrin.

The presence of CS increased the RAMEB solubilizing efficiency toward the drug of four times, accompanied, also in this case, by a stability constant reduction in OXA–RAMEB complex. Recent studies about the influence of CS on cyclodextrin complexing and solubilizing abilities showed that the presence of this polymer reduced the cyclodextrin complexing power toward various drugs, irrespective of their different physicochemical properties [46]. This was ascribed to the formation of interactions between CS and cyclodextrin, which hindered the drug–cyclodextrin complexation, thus giving rise to the association constant reduction. On the contrary, the influence of CS on the cyclodextrin solubilizing power depended on the drug type; in fact, both favorable (as in the present case) or negative or no effects have been obtained [20,21,46]. The concurrent formation of particular drug–CS and/or CS–(drug–cyclodextrin complex) interactions, distinct for each drug type, was regarded accountable for these different findings [46].

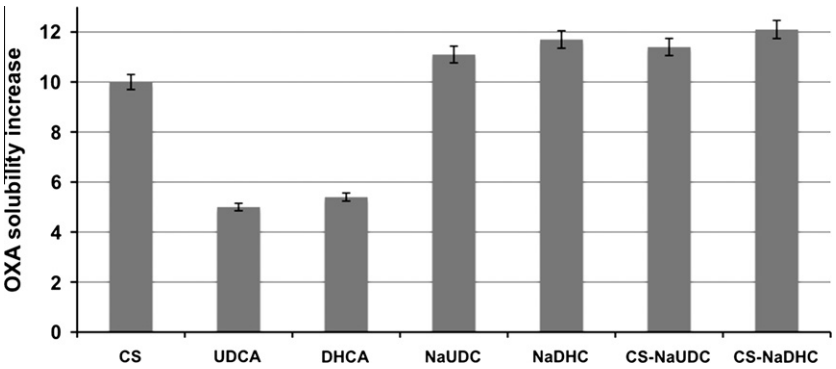

Fig. 2. Relative solubility increase of oxaprozin in pH 5.5 phosphate buffer solutions at 25 °C, in the presence of 0.0625% w/v of chitosan (CS), and/or of 2.5 mM bile acids (UDCA or DHCA) or salts (NaUDC). Each point represents the mean of three determinations (CV < 3%).

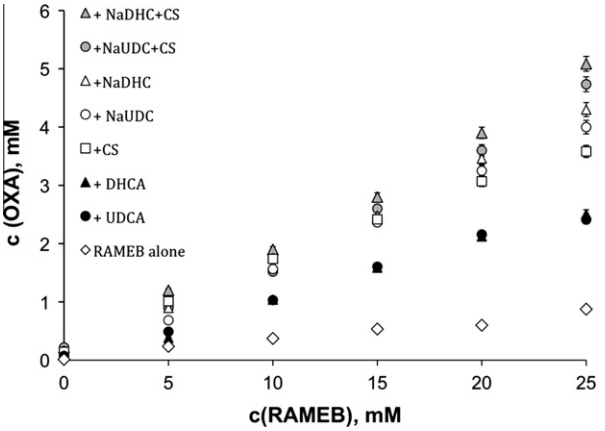

Fig. 3. Effect of increasing concentrations of RAMEB, alone or in the presence of 0.0625% w/v of chitosan (CS), and/or of 2.5 mM bile acids (UDCA or DHCA) or salts (NaUDC or NaHDC) on oxaprozin (OXA) solubility in pH 5.5 phosphate buffer solutions at 25 °C. Each point represents the mean of three determinations (CV < 3%).

Table 1
Apparent stability constants of 1:1 complexes ($K_{1:1}$) of oxaprozin with RAMEB, alone or in the presence of CS (0.0625% w/v) and/or bile components (2.5 mM).

Sample	$K_{1:1}$ (M^{-1})	Solubilizing efficiency[a]
RAMEB	2340	62.6
RAMEB + CS	1110	255.9
RAMEB + UDCA	1520	141.3
RAMEB + DHCA	1410	179.0
RAMEB + NaUDC	1210	285.6
RAMEB + NaDHC	1110	307.2
RAMEB + CS + NaUDC	900	338.1
RAMEB + CS + NaDHC	1070	363.2

[a] Ratio between solubility of drug in the presence of 25 mM RAMEB and/or other components and drug alone in pH 5.5 phosphate buffer at 25 °C.

A further improvement of RAMEB solubilizing efficiency was obtained in the simultaneous presence of CS and bile salts (Table 1). Therefore, drug–RAMEB–CS systems, with and without NaDHC or NaUDC, were selected to continue the study.

3.2. Characterization of solid systems

Drug–RAMEB–CS solid systems (with or without NaDHC or NaUDC) were prepared by physical mixing, co-grinding, kneading, coevaporation, and sealed-heating, in order to investigate the influence of the preparation method on the final product performance. The DSC curves of pure components and of the products obtained with the different techniques are shown in Fig. 4. The thermal curve of OXA was typical of a crystalline anhydrous substance, exhibiting an initial flat profile followed by a sharp and intense melting peak at 161.3 °C (ΔH_{fus} = 121.6 J/g). CS, RAMEB, and NaDHC revealed a thermal behavior representative of amorphous hydrated substances, displaying only a broad endothermal effect ascribed to water loss. The DSC curve of NaUDC presented instead, after the dehydration band between 70 and 100 °C, a broad fusion peak at 117.1 °C (ΔH_{fus} = 22.9 J/g).

In the OXA–RAMEB–CS series, the drug melting peak was still evident in the physical mixture (T_{peak} 145.7 ΔH_{fus} = 39.25 J/g), while it was scarcely detectable in the kneaded product (T_{peak} 130.24, ΔH_{fus} 8.82 J/g) and completely disappeared in all other systems, indicative of progressive drug amorphization as a consequence of interactions between the components. The whole absence of the drug fusion peak was observed in the DSC curves of all products of both the series containing the bile salts, except in the case of physical mixtures with RAMEB–CS–NaUDC, where the melting phenomena of both OXA and NaUDC were still detectable even if at lower temperature and with reduced enthalpy (T_{peak} NaUDC 113.8 °C, ΔH_{fus} = 3.39 J/g; T_{peak} OXA 140.0 °C; ΔH_{fus} = 11.7 J/g).

DSC analysis was also used to monitor the physical chemical stability of the different products stored one year under ambient conditions, in closed glass vials preserved from light. In all cases, no appreciable modifications in the DSC profiles were observed at the end of the storage period, indicating the stability of all the samples, and, in particular, the absence of possible drug recrystallization phenomena and of hygroscopicity problems.

Morphological evaluation of samples, performed by SEM analysis, confirmed DSC results, as shown in Fig. 5 for the selected series of OXA–RAMEB–CS systems. OXA particles appeared as oblong polyhedric crystals with smooth surfaces, while RAMEB looked as amorphous spherical particles and CS as amorphous flakes of rather irregular size. The typical drug crystals, mixed with particles of both RAMEB and CS, were clearly detectable in the physical mixture (Fig. 5D), whereas the morphology of both drug and carriers changed in co-ground and coevaporated products (Fig. 5E and F), where it was no more possible to distinguish the single components.

3.3. Dissolution studies

The drug dissolution curves from OXA–RAMEB–CS systems obtained by different preparation methods are shown in Fig. 6, while the related dissolution parameters are collected in Table 2. It is evident that all ternary systems showed very better dissolution properties than drug alone, and the extent of this effect significantly depended ($P < 0.05$) on the system preparation method. In particular, the observed improvement (in terms of both initial percent dissolved and dissolution efficiency at the end of the test) ranged from a minimum of about 8 times for physical mixtures up to a maximum of about 33 times for co-ground products. These results were consistent with those previously obtained for a series of binary systems of OXA with different cyclodextrins [9], thus confirming the importance of the binary system preparation method on the performance of the obtained product. Moreover, the CS presence greatly improved the RAMEB solubilizing efficacy toward OXA with respect to the corresponding OXA–RAMEB binary systems [9], thus corroborating the results of phase solubility studies. Co-grinding method confirmed its great effectiveness in establishing powerful solid-state interactions between the components [47], giving rise to the product with best dissolution behavior. For this reason, co-ground products of systems containing bile salts were selected for dissolution studies, in comparison with the corresponding physical mixtures (Fig. 7 and Table 2). The drug dissolution behavior from the different physical mixtures was practically the same, regardless of the presence and/or the type of bile salt. On the contrary, the co-ground product containing NaDHC showed significantly better dissolution properties ($P < 0.05$) than the corresponding product with NaUDC and also better ($P < 0.05$) than the drug–RAMEB–CS co-ground system, giving rise, respectively, to a 40 and 45 times increase of $DP_{10\%}$ and DE_{60} values with respect to the plain drug. The results were consistent with the higher solubilizing efficacy of NaDHC than NaUDC toward the drug, as found in phase solubility studies.

However, in spite of the more than 40 times increase in both percent drug dissolved at 10 min and DE_{60} values obtained with the best product, i.e., the OXA–RAMEB–CS–NaDHC co-ground system, it was not enough to allow drug promotion to BCS Class I. In fact, the OXA equilibrium solubility achieved with this system was 0.324 mg/mL, clearly still lower than its dose-relative

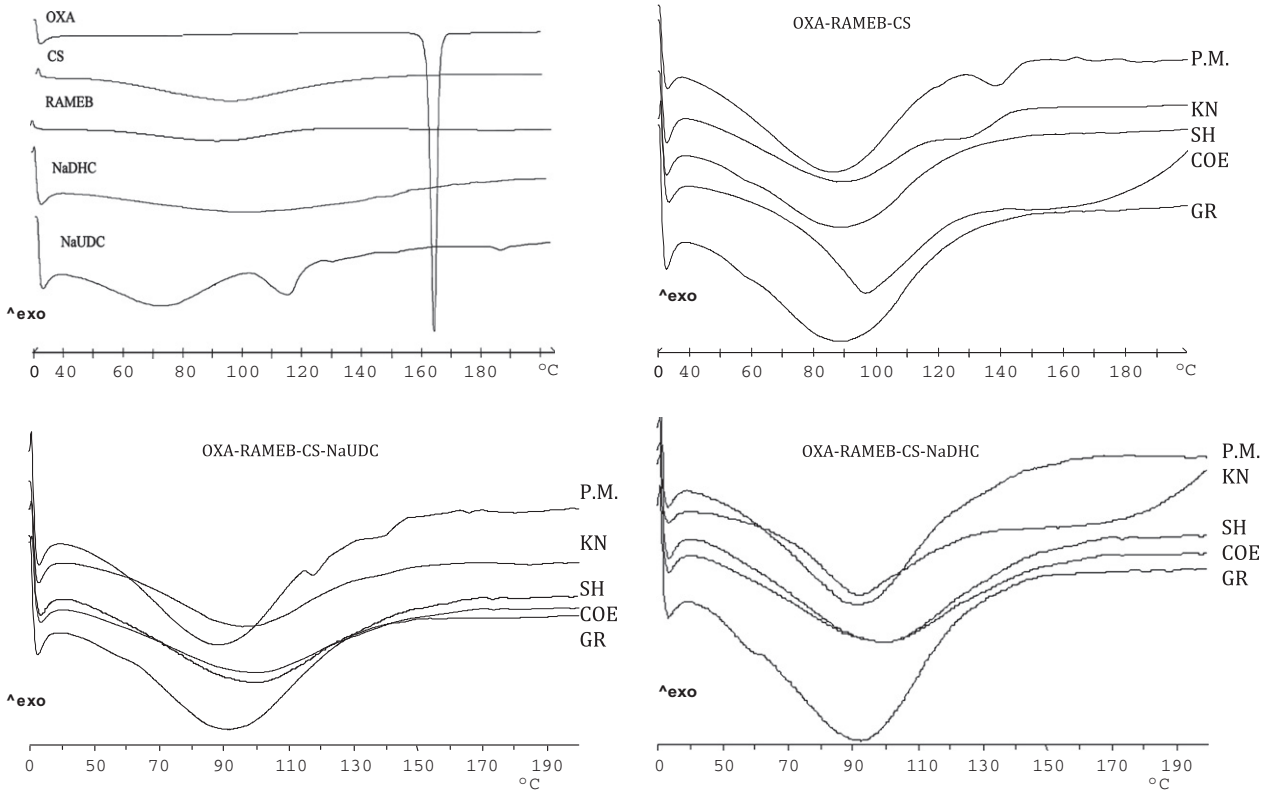

Fig. 4. DSC curves of pure components and of their physical mixtures (PM), kneaded (KN), sealed-heated (SH), coevaporated (COE), and co-ground (GR) products.

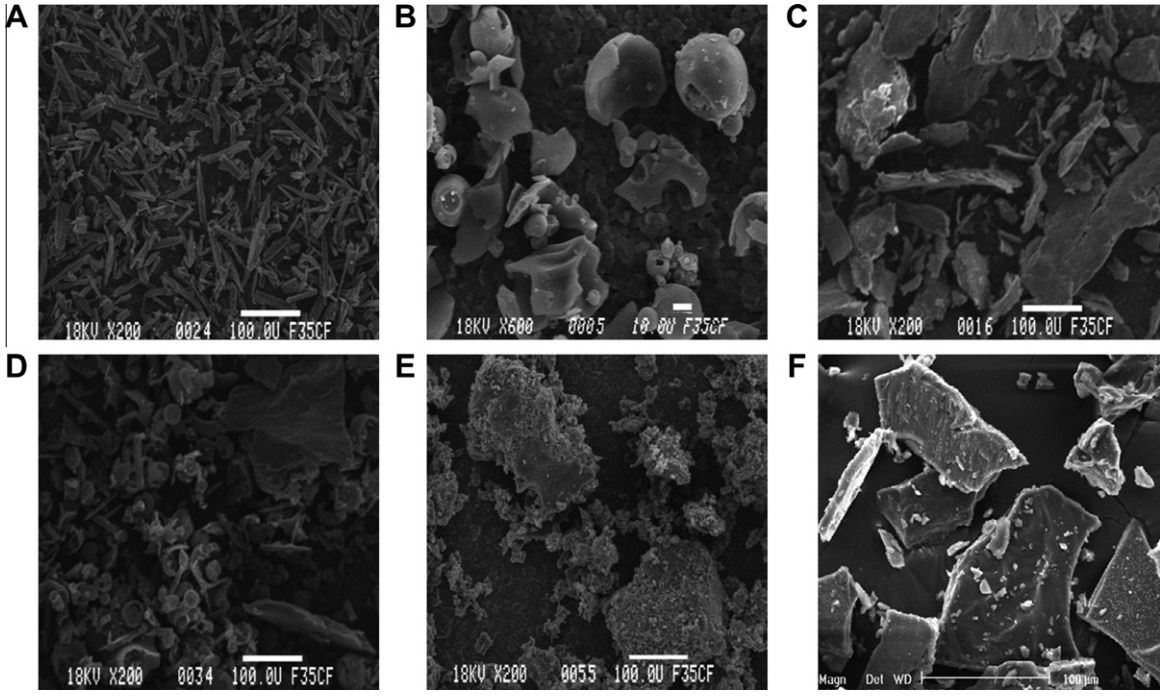

Fig. 5. SEM micrographs of pure oxaprozin (A), RAMEB (B), and chitosan (C), and their physical mixture (D), co-ground (E), and coevaporated (F) products.

solubility, calculated according to the FDA guidelines (considering the usual OXA dosage of 600 mg and a medium volume of 250 mL), which is 2.4 mg/mL. However, it is reasonable to suppose that the strong improvement obtained in drug solubility should allow a reduction in its dosage, and consequently, a further approaching to satisfy BCS Class I solubility conditions.

The dissolution profiles of OXA–RAMEB–CS co-ground products, containing or not NaDHC or NaUDC, after one year storage under ambient conditions in closed glass vials preserved from light, were not significantly different in terms of both percent dissolved drug ($P > 0.05$) and dissolution efficiency values ($P > 0.05$) from those of the corresponding freshly prepared products (data not shown).

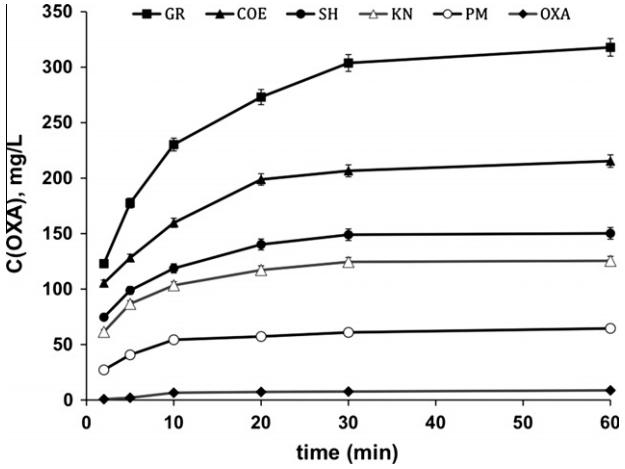

Fig. 6. Dissolution curves of oxaprozin (OXA) alone and from its physical mixture (PM), kneaded (KN), sealed-heated (SH), coevaporated (COE), and co-ground (GR) products with RAMEB and chitosan (CS). Each point represents the mean of four determinations (CV < 2.5%).

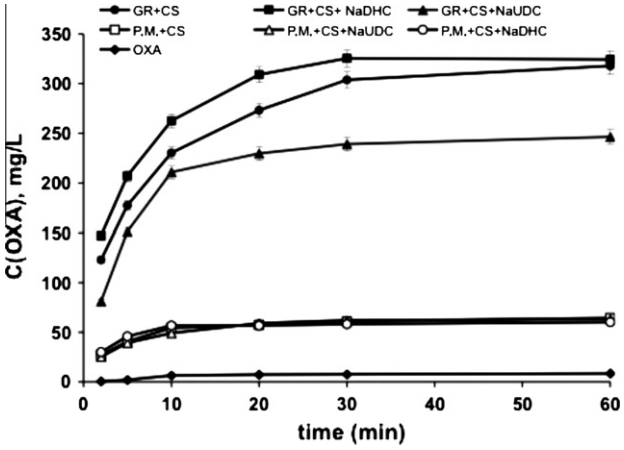

Fig. 7. Dissolution curves of oxaprozin (OXA) alone and from its physical mixtures (PM) or co-ground products (GR) with RAMEB and CS, in the presence or not of NaDHC. Each point represents the mean of four determinations (CV < 2.5%).

This confirmed the physical stability of the products and proved that the increased drug dissolution rate was maintained over the entire storage period.

3.4. Permeability studies

OXA–RAMEB–CS, OXA–RAMEB–CS–NaDHC co-ground products, resulted as the most effective systems in improving drug dissolution properties, were then selected, together with their corresponding physical mixtures, for performing transport studies across Caco-2 cells, in order to evaluate their possible effect on drug permeability. Binary OXA–RAMEB co-ground systems were also tested for comparison purposes.

The Caco-2 cell line was selected for this study since it showed to be a valuable model for evaluation of absorption enhancers. In particular, it has been successfully used for investigating the possible effect of CS [15,35,36,48], bile salts [22,49], or cyclodextrins [50,51] on drug absorption promotion.

LDH test, performed to evaluate the cytotoxicity of the tested carriers, evidenced that, at the used concentration, no one of the used carriers was cytotoxic. In fact, values of cellular damage higher than 20% were never observed, which corresponded to about 100% of cell survival determined by mitochondrial dehydrogenase activity (MTT test) [53].

In all the experiments, the transport of the drug was linear over the time period studied. TEER measurements, performed to verify the tightness of the junctions between cells [40], showed that no cellular damage occurred during the experiments. In fact, the final TEER values after 150 min never were below 200 $\Omega\,cm^2$ (with a variation lower than 20% with respect to the initial values), indicative of the integrity of the cell monolayers [52]. The mass balance was checked, and in all cases, it was higher than 90%.

The AP-to-BL apparent permeability values of OXA, alone or in its combinations with the examined carriers, calculated from the slopes of permeation profiles at 37 °C, are shown in Table 3, together with the corresponding apparent permeability values of Yellow Lucifer obtained in the same experiments. No significant Papp variation ($P > 0.05$) with respect to the drug alone was found for OXA equimolar binary combination with RAMEB. This result suggested that, at the used concentration, RAMEB simply acted as a solubility enhancer and did not reveal any significant effect in opening epithelial tight junctions, as confirmed by the lack of improvement of the hydrophilic marker flux.

On the contrary, a significant ($P < 0.05$) 1.6-fold increase in drug permeability was observed in systems containing RAMEB–CS combinations. The positive influence of CS could be due to its marked mucoadhesive properties, allowing a better and more prolonged drug contact with the cellular membranes. Moreover, CS was also able to significantly ($P < 0.05$) increase the Yellow Lucifer permeability through Caco-2 monolayers, probably as a consequence of reversible tight junctions opening [15]. Then, also this effect could lead to the observed transport increase in the drug through the epithelial cells. The better effect of RAMEB–CS co-administration, with respect to RAMEB alone, in promoting drug absorption has been previously reported for other drugs, such as estradiol [19] or gliburide [21]. The authors explained the obtained absorption enhancement with a combined mechanism: at first CS interacts with the epithelial cells, producing the tight junctions opening,

Table 2
Percent dissolved at 10 min and dissolution efficiency at 60 min, and ratio test values of OXA alone and from its physical mixtures (PM), kneaded (KN), sealed-heated (SH), coevaporated (COE), and co-ground (GR) products with RAMEB, CS, and bile salts (mean ± SD, $n = 4$).

Sample	$DP_{10\%}$	DE_{60}	$DP_{10\%}$ ratio	$DE_{60\%}$ ratio
OXA	0.98 ± 0.02	1.03 ± 0.03	–	–
PM OXA–RAMEB–CS	8.14 ± 0.19	8.48 ± 0.21	8.3	8.2
KN OXA–RAMEB–CS	15.51 ± 0.36	17.05 ± 0.38	15.8	16.5
SH OXA–RAMEB–CS	17.79 ± 0.43	20.27 ± 0.48	18.1	19.7
COE OXA–RAMEB–CS	23.96 ± 0.58	28.32 ± 0.64	24.4	27.5
GR OXA–RAMEB–CS	32.94 ± 0.75	39.80 ± 0.99	33.6	38.6
PM OXA–RAMEB–CS–NaUDC	7.35 ± 0.17	8.43 ± 0.20	7.5	8.2
GR OXA–RAMEB–CS–NaUDC	35.93 ± 0.78	42.79 ± 0.80	36.7	41.5
PM OXA–RAMEB–CS–NaDHC	8.67 ± 0.18	8.30 ± 0.19	8.8	8.1
GR OXA–RAMEB–CS–NaDHC	39.40 ± 0.95	45.90 ± 1.05	40.2	44.6

Table 3
Apparent permeability (Papp) values across Caco-2 cells at 37 °C of oxaprozin (OXA) alone and from its physical mixtures (PM) and co-ground (GR) products with RAMEB, CS, and NaDHC and corresponding values of Yellow Lucifer (YL) Papp ($n = 6$, standard deviations in brackets).

Sample	OXA Papp 10^{-5} (cm/s)	YL Papp 10^{-6} (cm/s)
OXA	2.32 (0.08)	1.12 (0.03)
GR OXA–RAMEB	2.44 (0.09)	1.15 (0.04)
PM OXA–RAMEB–CS	3.79 (0.30)[a]	1.71 (0.12)[a]
GR OXA–RAMEB–CS	3.86 (0.24)[a]	1.75 (0.15)[a]
PM OXA–RAMEB–CS–NaDHC	5.00 (0.26)[a,b]	2.42 (0.21)[a,b]
GR OXA–RAMEB–CS–NaDHC	5.33 (0.34)[a,b]	2.45 (0.25)[a,b]

[a] Significantly different ($P < 0.05$) from OXA alone.
[b] Significantly different ($P < 0.05$) from the corresponding sample without NaDHC.

and then RAMEB could more effectively penetrate and extract the phospholipids from bio-membranes, thus temporarily lowering their resistance [19].

Moreover, very interesting results were obtained with combinations containing the bile salt. In fact, the simultaneous presence of CS and NaDHC showed a synergistic effect, giving rise to a 2.3-fold increase in drug permeability with respect to OXA alone and a significant ($P < 0.05$) 1.4-fold increase with respect to the corresponding systems without NaDHC, accompanied by a further parallel improvement in the hydrophilic marker permeability (Table 3). However, differently from previous studies on naproxen–CS systems [37], where co-ground products were clearly more effective than physical mixtures in improving drug permeation, suggesting that the co-grinding treatment gave rise to an activated, more permeable form of the drug, in the present case, no significant differences were found between co-ground and simply blended products. Evidently, the improvement in OXA permeation rate was due to the intrinsic permeability enhancer effect of the carriers, and not to the presence of drug-carrier interactions, brought about during the co-grinding process, which, on the contrary, were responsible for the improved drug dissolution rate (Table 2).

4. Conclusion

This study demonstrated that CS addition improved the RAMEB effectiveness in enhancing OXA dissolution behavior. Moreover, the preparation technique of OXA–CS–RAMEB ternary products highly affected the drug dissolution performance, and co-ground products gave the best results.

In the same way, OXA–CS–RAMEB systems showed significantly better ($P < 0.05$) drug permeation properties through Caco-2 cells than the corresponding OXA–RAMEB systems. However, in this case, the effect was directly related to the presence of the carriers, irrespective of the sample preparation method.

Interestingly, the addition of NaDHC to OXA–CS–RAMEB systems not only improved drug solubility and dissolution rate, in virtue of the surfactant and wetting properties of bile salts, but also gave rise to an about 40% drug permeability increase with respect to the corresponding sample without bile salt, revealing a synergistic enhancer effect between NaDHC and CS.

The obtained results suggested that the use of proper combinations of RAMEB, CS, and NaDHC could be opportunely exploited to develop suitable oral dosage forms of OXA, able to simultaneously improve drug solubility and permeability, and, consequently, enhance and make less variable its bioavailability, and reduce dose-related side effects.

Finally, based on these findings, it could be envisaged that this proposed carrier combination could find other useful application as general enhancer of drug intestinal absorption.

Acknowledgments

The support of Professor Renè Li-Khuan (Faculté de Sciences Pharmaceutiques et Biologiques, Université de Paris V, Paris, France) for scanning electron microscopy analysis is gratefully acknowledged. Financial support from MIUR is acknowledged.

References

[1] G.L. Amidon, H. Lennernäs, V.P. Shah, J.R. Crison, A theoretical basis for a biopharmaceutic drug classification: the correlation of in vitro drug product dissolution and in vivo bioavailability, Pharm. Res. 12 (1995) 413–420.
[2] R.A. Löbenberg, G.L. Amidon, Modern bioavailability, bioequivalence and biopharmaceutics classification system. New scientific approaches to international regulatory standards, Eur. J. Pharm. Biopharm. 50 (2000) 3–12.
[3] L.X. Yu, G.L. Amidon, J. Polli, E.H. Zhao, M.U. Mehta, D.P. Conner, V.P. Shah, L.C.J. Lesko, L.V. Mei-Ling, A.S. Hussain, Biopharmaceutics classification system: the scientific basis for biowaiver extensions, Pharm. Res. 19 (2002) 921–925.
[4] M. Kansy, F. Senner, K. Gubernator, Physicochemical high throughput screening: parallel artificial membrane permeation assay in the description of passive absorption processes, J. Med. Chem. 41 (1998) 1007–1010.
[5] V.K. Gombar, I.S. Silver, Z. Zhao, Role of ADME characteristics in drug discovery and their in silico evaluation: in silico screening of chemicals for their metabolic stability, Curr. Top. Med. Chem. 3 (2003) 1205–1225.
[6] C.A. Lipinski, F. Lombardo, B.W. Dominy, P.J. Feeney, Experimental and computational approaches to estimate solubility and permeability in drug discovery and development settings, Adv. Drug Del. Rev. 46 (2001) 3–26.
[7] M. Yazdanian, K. Briggs, C. Jankovsky, A. Hawi, The high solubility definition of the current FDA guidance on biopharmaceutical classification system may be too strict for acidic drugs, Pharm. Res. 21 (2004) 293–299.
[8] R. Rothstein, Safety profiles of leading nonsteroidal anti-inflammatory drugs, Am. J. Med. 105 (1998) 39–43.
[9] F. Maestrelli, M. Cecchi, M. Cirri, G. Capasso, N. Mennini, P. Mura, Comparative study of oxaprozin complexation with natural and chemically modified cyclodextrin in solution and in the solid state, J. Incl. Phenom. Macrocycl. Chem. 63 (2009) 17–25.
[10] T. Kiss, F. Fenyvesi, I. Bacskay, J. Varadi, E. Fenyvesi, R. Ivanyi, L. Szente, A. Tosaki, M. Vecsernyes, Evaluation of cytotoxicity of β-cyclodextrin derivatives: evidence for the role of cholesterol extraction, Eur. J. Pharm. Sci. 40 (2010) 376–380.
[11] T. Loftsson, H. Fridriksdóttir, A.M. Sigurdardóttir, H. Ueda, The effect of water-soluble polymers on drug–cyclodextrin complexation, Int. J. Pharm. 110 (1994) 169–177.
[12] T. Loftsson, M. Brewster, Pharmaceutical applications of cyclodextrins. 1. Drug solubilization and stabilization, J. Pharm. Sci. 85 (1996) 1017–1025.
[13] G. Ganzerli, L. van Santvliet, E. Verschuren, A. Ludwig, Influence of beta-cyclodextrin and various polysaccharides on the solubility of fluorescein and on the rheological and mucoadhesive properties of ophtalmic solutions, Pharmazie 51 (1996) 357–362.
[14] P. Mura, M.T. Faucci, G.P. Bettinetti, The effect of polyvinylpyrrolidone on hydroxypropyl-β-cyclodextrin complexation with naproxen, Eur. J. Pharm. Sci. 13 (2001) 187–194.
[15] L. Illum, Chitosan and its use as a pharmaceutical excipient, Pharm. Res. 15 (1998) 1326–1331.
[16] A. Portero, C. Remuñan-Lopez, J.L. Vila-Jato, Effect of chitosan and chitosan glutamate enhancing the dissolution properties of the poorly water soluble drug nifedipine, Int. J. Pharm. 175 (1998) 75–84.
[17] W. Paul, C.P. Sharma, Chitosan, a drug carrier for the 21st century, STP Pharma Sci. 10 (2000) 5–22.
[18] M. Açikgoz, H.S. Kas, Z. Hasçelik, U. Milli, A.A. Hincal, Chitosan microspheres of diclophenac sodium, II: in vitro and in vivo evaluation, Pharmazie 50 (1995) 275–277.
[19] W. Leng, L. Qin, X. Tang, Chitosan and randomly methylated β-cyclodextrin combine to enhance the absorption and elevate the bioavailability of estradiol intranasally: in situ and in vivo studies, J. Am. Sci. 2 (2006) 61–65.
[20] F. Maestrelli, M. Garcia-Fuentes, P. Mura, M.J. Alonso, A new drug nanocarrier consisting of chitosan and hydroxypropylcyclodextrin, Eur. J. Pharm. Biopharm. 63 (2006) 79–86.
[21] N. Zerrouk, G. Corti, S. Ancillotti, F. Maestrelli, M. Cirri, P. Mura, Influence of cyclodextrins and chitosan, separately or in combination, on glyburide solubility and permeability, Eur. J. Pharm. Biopharm. 62 (2006) 241–246.
[22] C.M. Meaney, C.M. O'Driscoll, A comparison of the permeation enhancement potential of simple bile salt and mixed bile salt:fatty acid micellar systems using the CaCo-2 cell culture model, Int. J. Pharm. 207 (2000) 21–30.
[23] S. Selvam, M.E. Andrews, A.K. Mishra, A photophysical study on the role of bile salt hydrophobicity in solubilizing amphotericin B aggregates, J. Pharm. Sci. 98 (2009) 4153–4160.
[24] M. Atanacković, M. Poša, H. Heinle, L. Gojković-Bukarica, J. Cvejić, Solubilization of resveratrol in micellar solutions of different bile acids, Colloids Surf. B 72 (2009) 148–154.
[25] M. Almgren, Mixed micelles and other structures in the solubilization of bilayer lipid membranes by surfactants, Biochim. Biophys. Acta 1508 (2000) 146–163.

[26] P. Garidel, A. Hildebrand, K. Knauf, A. Blume, Membranolytic activity of bile salts: influence of biological membrane properties and composition, Molecules 12 (2007) 2292–2326.
[27] J.S. Dangi, S.P. Vyas, V.K. Dixit, Effect of various lipid–bile salt mixed micelles on the intestinal absorption of amphotericin-B in rats, Drug Dev. Ind. Pharm. 24 (1998) 631–635.
[28] P. Sharma, M.V.S. Varma, H.P.S. Chawla, R. Panchagnula, Relationship between lipophilicity of BCS class III and IV drugs and the functional activity of peroral absorption enhancers, Il Farmaco 60 (2005) 870–873.
[29] M. Miyake, T. Minami, M. Hirota, H. Toguchi, M. Odomi, K. Ogawara, K. Higaki, T. Kimura, Novel oral formulation safely improving intestinal absorption of poorly absorbable drugs: utilization of polyamines and bile acids, J. Control. Release 111 (2006) 27–34.
[30] Physician's Desk Reference, 55th ed. Medical Economic Co., Montvale, NJ, 1996.
[31] K. Matsuoka, Y. Moroi, Micelle formation of sodium deoxycholate and sodium ursodeoxycholate, Biochim. Biophys. Acta 1580 (2002) 189–199.
[32] A.F. Hofmann, K.J. Mysels, Bile acid solubility and precipitation in vitro and in vivo: the role of conjugation, pH, and Ca^{2+} ions, J. Lipid Res. 33 (1992) 617–626.
[33] T. Higuchi, K.A. Connors, Phase-solubility techniques, Adv. Anal. Chem. Instrum. 4 (1965) 117–212.
[34] K.A. Khan, The concept of dissolution efficiency, J. Pharm. Pharmacol. 27 (1975) 48–49.
[35] P. Costa, J.M. Sousa Lobo, Modeling and comparison of dissolution profiles, Eur. J. Pharm. Sci. 13 (2001) 123–133.
[36] F. Maestrelli, N. Zerrouk, C. Chemtob, P. Mura, Influence of chitosan and its glutamate and hydrochloride salts on naproxen dissolution rate and permeation across Caco-2 cells, Int. J. Pharm. 271 (2004) 257–267.
[37] G. Corti, F. Maestrelli, M. Cirri, P. Mura, N. Zerrouk, Dissolution and permeation properties of naproxen from solid-state systems with chitosan, Drug Deliv. 15 (2008) 303–312.
[38] A.F. Kotzé, B.J. de Leeuw, H.L. Lueßen, A.G. de Boer, J.C. Verhoef, H.E. Junginger, Chitosans for enhanced delivery of therapeutics peptides across intestinal epithelia: in vitro evaluation in Caco-2 cell monolayers, Int. J. Pharm. 159 (1997) 243–253.
[39] V. Pade, S. Stavchansky, Estimation of the relative contribution of the transcellular and paracellular pathway to the transport of passively absorbed drugs in the Caco-2 cell culture model, Pharm. Res. 14 (1997) 1210–1215.
[40] G. Borchard, H.L. Lueßen, A.G. de Boer, J.C. Verhoef, C. Lehr, H.E. Junginger, The potential of mucoadhesive polymer in enhancing intestinal peptide drug absorption. III: effect of chitosan-glutamate and carbomer on epithelial tight junction in vitro, J. Control. Release 39 (1996) 131–138.
[41] C. Korzeniewski, D.M. Callewaert, An enzyme-release assay for natural cytotoxicity, J. Immunol. Methods 64 (1983) 313–320.
[42] K.V. Reddy, D.S. Rao, K. Vyas, G.O. Reddy, LC method for the quantitative determination of oxaprozin and its impurities in the bulk drug, J. Pharm. Biomed. Anal. 22 (2000) 651–659.
[43] A. Tangerman, Van Schaik, E.W. Van drr Hoeck, Analysis of conjugated and unconjugated bile acid in serum and jejunal fluid of normal subjects, Clin. Chim. Acta 159 (1986) 123–132.
[44] A. Mucci, L. Schenetti, G. Salvioli, P. Ventura, M.A. Vandelli, F. Forni, The interaction of biliar acids with 2-hydroxypropyl-β-cyclodextrin in solution and in the solid state, J. Incl. Phenom. Mol. Recogn. Chem. 26 (1996) 233–241.
[45] P. Ramos Cabrer, E. Alvarez-Parrilla, W. Al-Soufi, F. Meijide, E. Rodriguez Nunez, J. Vàsquez Tato, Complexation of bile salts by natural cyclodextrins, Supramol. Chem. 15 (2003) 33–43.
[46] P. Mura, G. Corti, F. Maestrelli, M. Cirri, The influence of chitosan on cyclodextrin complexing and solubilizing abilities towards drugs, J. Incl. Phenom. Macrocycl. Chem. 59 (2007) 307–313.
[47] S. Lin, C. Hsu, M. Sheu, Curve-fitting FTIR studies of loratadine/hydroxypropyl-β-cyclodextrin inclusion complex induced by co-grinding process, J. Pharm. Biomed. Anal. 53 (2010) 799–803.
[48] P. Artursson, T. Lindmark, S.S. Davis, L. Illum, Effect of chitosan on the permeability of monolayers of intestinal epithelial cells (Caco2), Pharm. Res. 11 (1994) 1358–1361.
[49] Y.L. Lo, J.D. Huang, Effects of sodium deoxycholate and sodium caprate on the transport of epirubicin in human intestinal epithelial Caco-2 cell layers and everted gut sacs of rats, Biochem. Pharmacol. 59 (2000) 665–672.
[50] L. Hovgaard, H. Brondsted, Drug delivery studies in Caco-2 monolayers. IV. Absorption enhancer effects of cyclodextrins, Pharm. Res. 12 (1995) 1328–1332.
[51] H. Arima, K. Yunomae, F. Hirayama, K. Uekama, Contribution of P-glycoprotein to the enhancing effects of dimethyl-b-cyclodextrin on oral bioavailability of tacrolimus, J. Pharmacol. Exp. Ther. 297 (2001) 547–555.
[52] J. Phillips, A. Arena, Optimization of Caco-2 Cell Growth and Differentiation for Drug Transport Studies, Millipore Corporation Protocol Note PC1060EN00, 2003.
[53] H. Vihola, A. Laukkanen, L. Valtola, H. Tenhu, J. Hirvonen, Cytotoxicity of thermosensitive polymers poly(N-isopropylacrylamide), poly(N-vinylcaprolactam) and amphiphilically modified poly(N-vinylcaprolactam), Biomaterials 26 (2005) 3055–3064.